Atmospheric Science Letters (2001) Volume 1
doi:10.1006/asle.2001.0023

Biogeophysical impacts of land use on present-day climate: near-surface temperature change and radiative forcing

Richard A. Betts*

Met Office, Hadley Centre for Climate Prediction and Research, Bracknell, Berkshire RG12 2SY, U.K.

Abstract: Changes in land cover affect climate through the surface energy and moisture budgets, but these biogeophysical impacts of land use have not yet been included in General Circulation Model (GCM) simulations of 20th century climate change. Here, the importance of these effects was assessed by comparing climate simulations performed with current and potential natural vegetation. The northern mid-latitude agricultural regions were simulated to be approximately 1–2 K cooler in winter and spring in comparison with their previously forested state, due to deforestation increasing the surface albedo by approximately 0.1 during periods of snow cover. Some other regions such as the Sahel and India experienced a small warming due to land use. Although the annual mean global temperature is only 0.02 K lower in the simulation with present-day land use, the more local temperature changes in some regions are of a similar magnitude to those observed since 1860. The global mean radiative forcing by anthropogenic surface albedo change relative to the natural state is simulated to be -0.2 Wm^2, which is comparable with the estimated forcings relative to pre-industrial times by changes in stratospheric and tropospheric ozone, N_2O, halocarbons, and the direct effect of anthropogenic aerosols. Since over half of global deforestation has occurred since 1860, simulations of climate since that date should include the biogeophysical effects of land use.

Keywords: Climate change, land use, radiative forcing.

1. INTRODUCTION

Investigations of anthropogenic contributions to climate change typically consist of a comparison of the observational record against GCM simulations performed with a number of sources of forcing (Santer *et al.*, 1996; Tett *et al.*, 1999). Although the forcing by increasing greenhouse gas emissions includes a contribution from deforestation (Schimel *et al.*, 1996), this is only one means by which land cover change can influence climate. Vegetation also affects the surface fluxes of radiation, heat, moisture and momentum, so modifying the vegetation cover can change the lower boundary conditions of the atmosphere and hence impact the climate (Pielke *et al.*, 1998).

* Email: richard.betts@metoffice.com

1530-261X

Conversion of forest to arable land or pasture reduces the aerodynamic roughness of the landscape and decreases both the capture of precipitation on the canopy and the root extraction of soil moisture; these changes tend to decrease evaporation and hence the fluxes of moisture and latent heat from the surface to the atmosphere, and this acts to increase the temperature near the surface. Also, a forested landscape generally has a lower surface albedo than open land, particularly in conditions of lying snow when short-wave radiation is trapped by multiple reflections within the forest canopy. Deforestation can therefore lead to increased short-wave reflection, which provides a cooling influence. The relative importance of these processes depends on local conditions such as the underlying surface albedo and soil moisture availability, and can vary with season and location (Betts, 1999). Coarse-resolution simulations suggest that the biogeophysical effects of historical land cover change may have exerted significant impacts on the climate, with the main effect being a northern-hemisphere cooling attributed to increased surface albedo (Brovkin *et al.*, 1999). However, these effects have so far been neglected from higher-resolution GCM simulations designed to detect authropogenic climate change (Santer *et al.*, 1996). The present work aims to assess the importance of this omission.

Another tool used to compare the various human and natural drivers of climate change is the concept of radiative forcing (Houghton *et al.*, 1995). This can be thought of as a perturbation to the global radiation budget prior to any feedbacks resulting from the response of other aspects of the climate system, and is conventionally defined as the change in the net flux at the tropopause. Since the radiation budget is the fundamental driver of the climate system, the concept of radiative forcing can provide a useful indicator of the relative importance of the different mechanisms of climate change. Land-use-induced surface albedo change perturbs the radiation budget by modifying the absorption of short-wave radiation; this short-wave radiative forcing can then be compared with the radiative forcings by greenhouse gases, aerosols and solar output changes to assess the importance of surface albedo change in relation to these other climatic influences. Hence, a second aim of this work is to quantify the radiative forcing by surface albedo change since pre-agricultural times. Furthermore, since albedo change is merely one mechanism through which vegetation affects climate, a third aim is to assess whether the radiative forcing is a useful indicator of the influence of land use on present-day climate.

The 3rd Hadley Centre Atmospheric General Circulation Model (HadAM3) was used to simulate the climatic changes due to the change from natural vegetation to the present-day state. The results presented here concentrate on two aspects of the climate change; the near-surface temperature difference, and the radiative forcing.

2. CURRENT AND POTENTIAL VEGETATION DATASETS

Two datasets of global land cover were used, one representing actual present-day vegetation including agriculture (Wilson and Henderson-Sellers, 1985, hereafter "ACT" Figure 1a), and the other representing a return to the potential natural state ("NAT", Figure 1c). The two datasets used the land cover classification system of Wilson and Henderson-Sellers (1985) ("WHS"), which specifies 53 classes of vegetation and other land cover. The ACT dataset allocates up to two classes of land cover per 1° gridbox, a primary class covering 75% of the box and a secondary class covering 25%; this allows for a mixture of land cover types within a gridbox, which is important here since agriculture cover may be a significant portion of the landscape even if it is not the dominant land cover class.

The NAT dataset was constructed from ACT by replacing agricultural vegetation with natural vegetation through a combination of extrapolation and modelling. Each of the 53 WHS land cover classes was identified as either "natural" or "agricultural", and in each 1° gridbox in ACT any "agricultural" classes were removed. If only one of the two classes had been removed, the remaining class in the gridbox was assumed to represent the potential vegetation state of the entire gridbox, so the coverage of that class was set to 100%. If both

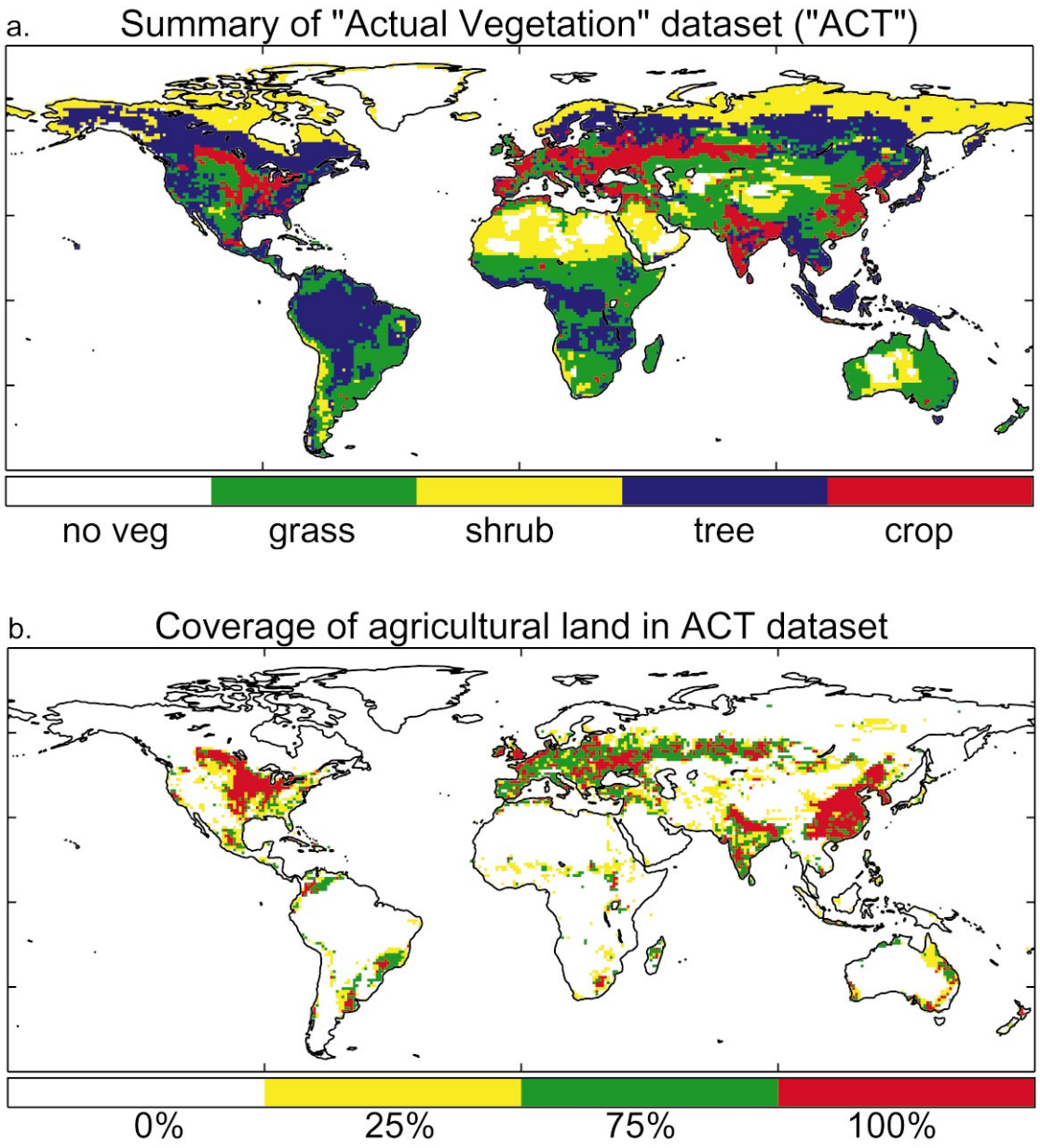

Figure 1a,b. Figure caption on page 4.

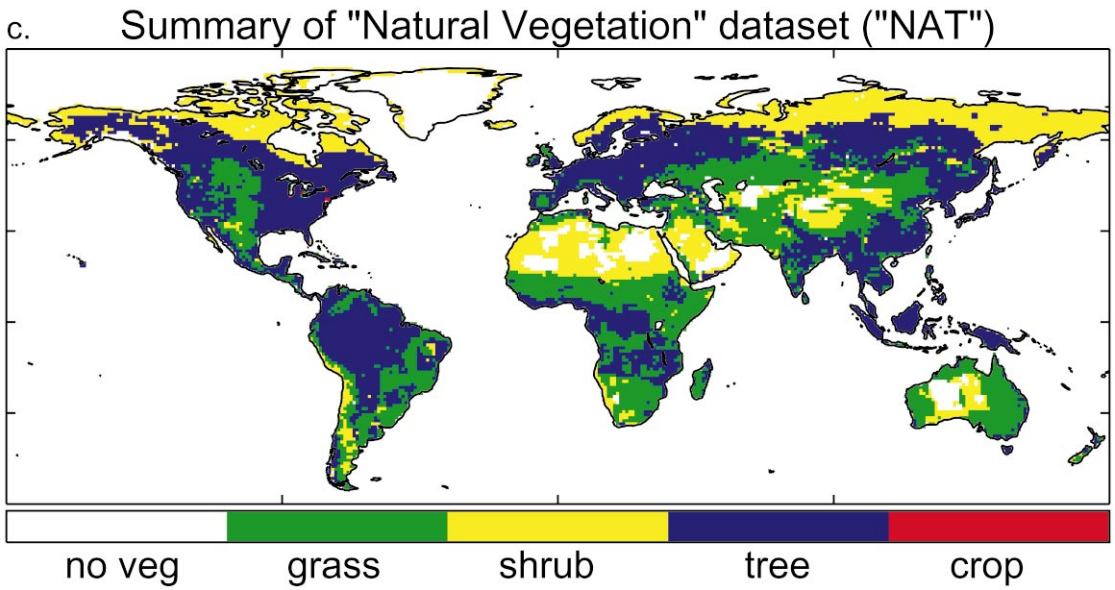

Figure 1. Vegetation datasets and extent of differences between them. (a) Summary of ACT dataset. Actual dataset consists of 53 land cover classes; for clarity, these are grouped here according to the dominant plant functional type. (b) Coverage of agricultural classes in ACT dataset. Agriculture covering less than 25% of a 1° gridbox is not resolved. (c) Summary of NAT dataset, with classes grouped as described in (a).

the primary and secondary class had been identified as agriculture and hence removed, the appropriate natural class for that gridbox was allocated by reference to plant functional types and leaf area index simulated by the Sheffield University vegetation model (Woodward *et al.*, 1995) driven by the observed present-day climate. In gridboxes where both primary and secondary classes were already ''natural'' in ACT, these were left unchanged for NAT. The resulting dataset of potential vegetation (Figure 1c) shows good qualitative agreement with another such dataset derived independently by Haxeltine and Prentice (1996).

Clearly, land-cover types covering less than 25% of a 1° gridbox will not be represented in the ACT dataset, so where less than 25% of the landscape is used by humans, this will not be resolved in these simulations. Although higher-resolution datasets exist which would allow such areas of land use to be represented, use of such a dataset in this study would also require information on pre-human vegetation at a comparable resolution if the effects of the fine detail were to be meaningful. High-resolution land-cover datasets will be crucial for time-dependent simulations of the climatic effects of land use change over recent decades, but for a sensitivity study such as that presented here, the coarse-resolution datasets should provide a useful first-order indication of the importance of land use in the global climate.

3. CLIMATE SIMULATIONS

HadAM3 simulates the atmospheric circulation on a global grid of 3.75° longitude by 2.5° latitude with 19 levels in the vertical (Cullen, 1993). It includes parametrization schemes for the sub-gridscale processes of radiative transfer (Edwards and Slingo, 1996), cloud (Smith, 1990) (distinguishing convective and layer cloud), precipitation (Gregory and Mitchell, 1995) (distinguishing rain and snow), boundary layer turbulence (Smith, 1990), gravity wave drag (Gregory *et al.*, 1998) and surface hydrology (Cox *et al.*, 1999). The model timestep is 30 minutes, but for computational efficiency the radiation calculations are performed every sixth timestep with the radiative fluxes being adjusted for the solar zenith angle on other timesteps.

Simulation of the surface shortwave radiation budget includes a spatially-explicit surface albedo calculation which depends on the local vegetation and soil types and the depth and temperature of any lying snow (Hansen *et al.*, 1983). Of particular importance here is the inclusion of the effect of vegetation on surface albedo in snowy conditions (Thomas and Rowntree, 1992). Each vegetation type is allocated a separate albedo parameter for snow-free and deep-snow conditions (Cox *et al.*, 1999), and the latter provides an upper limit on the modelled surface albedo which increases with snow depth. The surface albedo calculated for a given location in snowy conditions can vary from 0.8 to 0.25 according to whether the local vegetation is farmland or forest.

Other vegetation-dependent parameters are root depth, which determines the depth to which soil moisture is available for transpiration; aerodynamic roughness, which represents the frictional effect of the surface on boundary layer flow; canopy water capacity, which specifies the maximum quantity of water that can be held on the canopy; the leaf area index, which is the ratio of leaf area to ground area; canopy height; fractional vegetation cover; and a surface water infiltration enhancement factor, which represents the effect of an ecosystem on soil porosity through the action of plant roots and soil organisms. In the standard HadAM3 configuration, the land surface characteristics are specified using the ACT land cover dataset. The surface fluxes of heat and moisture are simulated with the MOSES land surface scheme (Cox *et al.*, 1999). This uses the Penman-Monteith equation for evapotranspiration with interactive stomatal resistance (Cox *et al.*, 1998), and a four-layer Clapp-Hornberger soil hydrology module with soil moisture phase change included.

Three climate simulations were performed, all with the present-day atmospheric CO_2 concentration but each including different land surface parameter fields. In the first simulation all vegetation parameters were derived from the NAT dataset, while in the second simulation all parameters were derived from ACT. The difference between these two simulations therefore shows the effect of current land use on the model climate via the changes in the physical properties of the land surface (Figure 2). In the third simulation, only the albedo parameters were derived from NAT while the rest were derived from ACT; comparison of this simulation (ALBNAT) with the ACT climate isolates the climatic impact of the albedo change from that of the other surface properties.

To allow diagnosis of the radiative forcing by the albedo change, the simulation with ACT land cover also included an additional set of radiation calculations using the NAT albedo parameters. These calculations were performed on all radiation timesteps in parallel with those performed with the ACT parameters, using the same input variables but without passing the results to the rest of the model. This provided a simulation of the surface albedo and shortwave radiation fluxes with natural land cover but with present-day meteorological and hydrological conditions. By comparing these fluxes with those simulated with the ACT parameters, the direct effect of the land cover change could be distinguished from the indirect effects such as changes in snow and cloud cover; this therefore allowed separation of the forcing from the feedback. The difference in the outgoing shortwave radiation flux at the tropopause provided the instantaneous radiative forcing due to the albedo change.

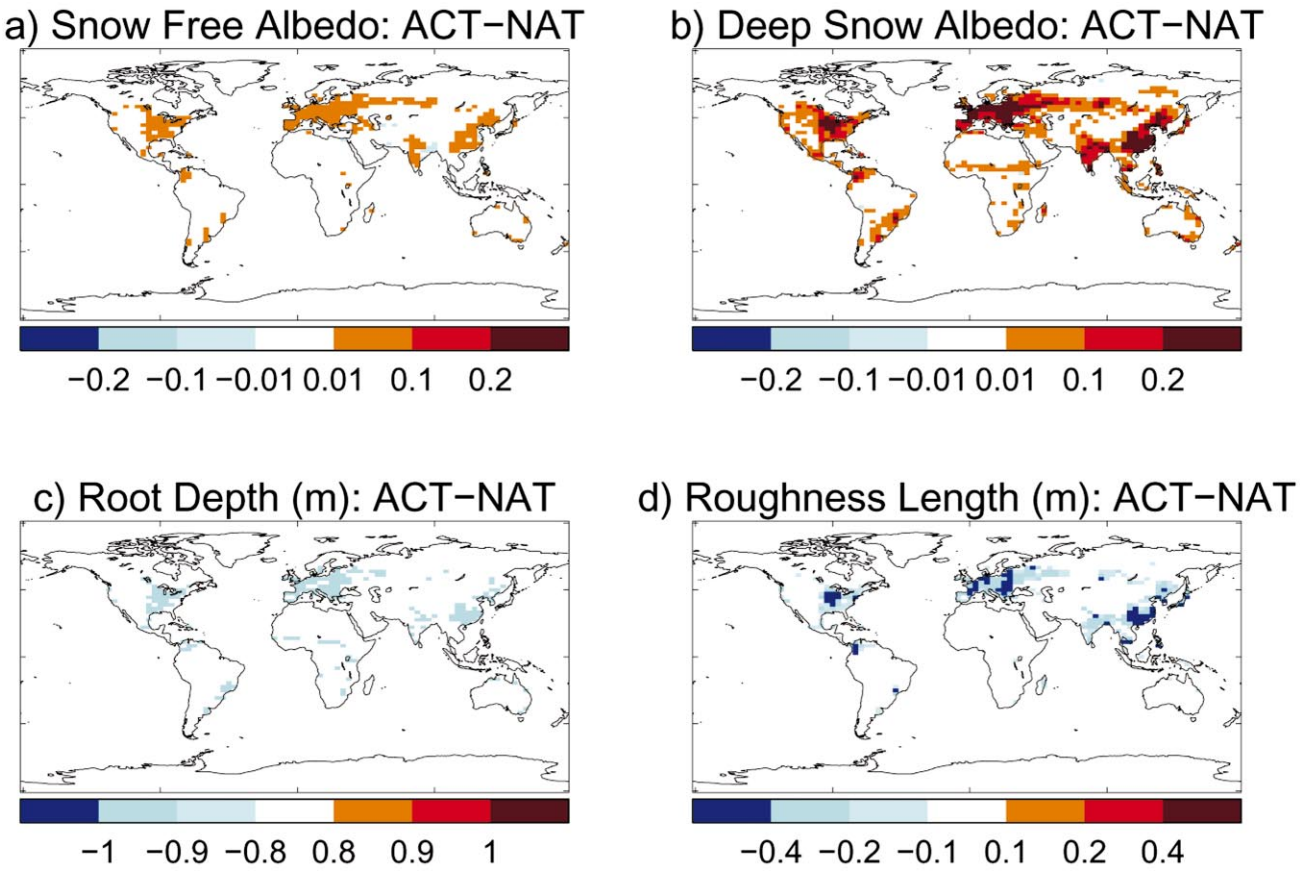

Figure 2a-d. Figure caption on page 7.

The simulations were run for twenty years, each having undergone a five-year spinup period, and the results presented here are twenty-year means. Simulations of this length were necessary to minimise the impact of internal variability in the model climate; it was found that a few anomalous years could dominate the results if only ten years of simulation were analysed. Sea-surface temperatures and sea ice cover were prescribed to present-day climatologies in all three simulations.

4. RESULTS

The largest and most extensive temperature changes occurred in the temperate agricultural regions in the northern winter and spring (Figure 3). In central North America, the Eurasian agricultural belt and China, temperatures at 1.5m above the surface were 1–2 K lower

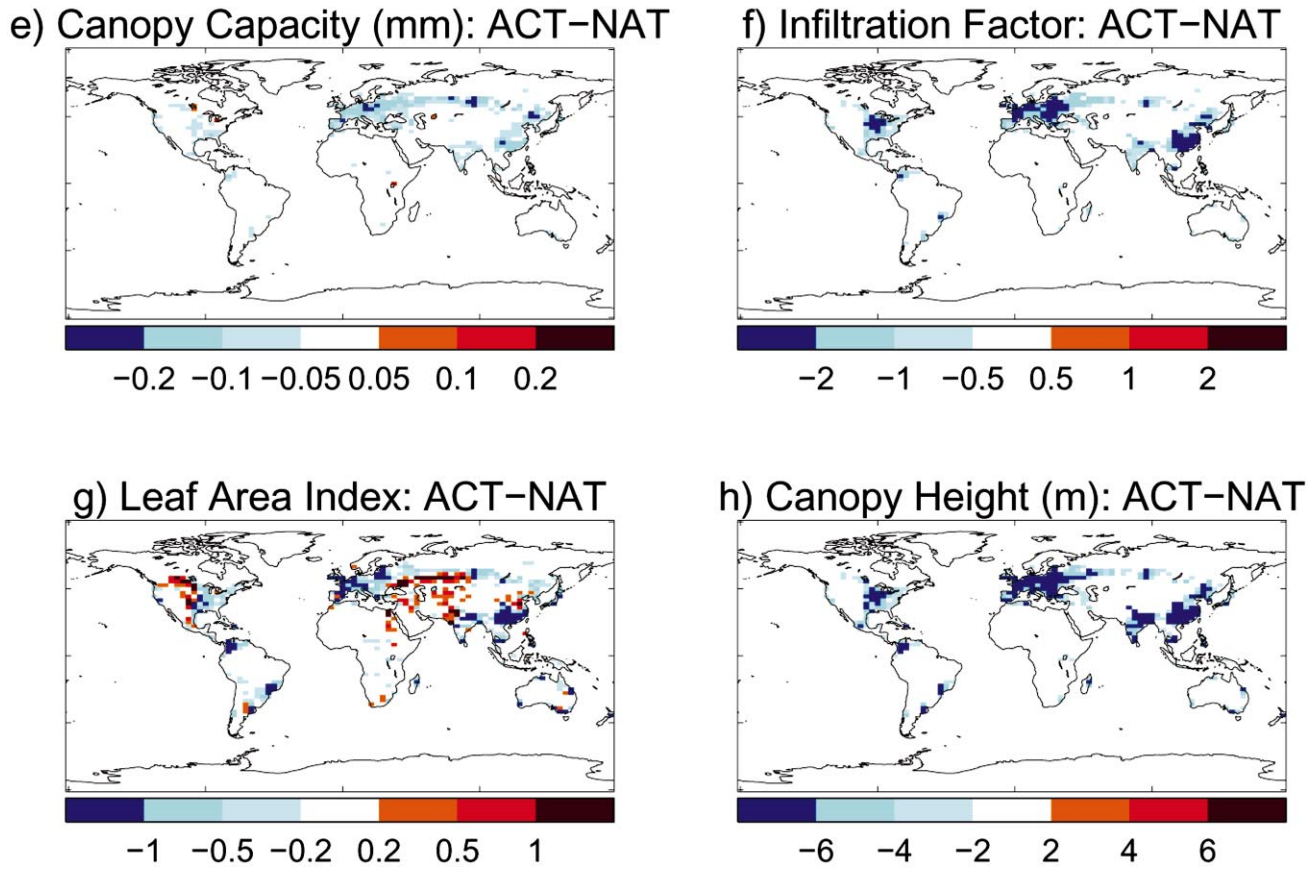

Figure 2. Differences in land surface parameter values, ACT-NAT.

with ACT than with NAT in December, January and February (DJF), and March, April and May (MAM). The simulated surface albedo was higher by 0.1 or more with ACT in these seasons, as a result of lying snow remaining exposed in the deforested areas. A similar albedo increase and temperature reduction was seen when comparing the ACT climate with ALBNAT (Figure 4), which suggests that this surface albedo difference was the main driver of the temperature change in these regions during this part of the year. Although the albedo difference was greatest in DJF, the impact on the net surface shortwave radiation flux and surface temperature was greater in MAM when the solar zenith angle is smaller. In the annual mean, temperature changes of −0.5 K to −1 K were seen in these areas (Figure 5a). This GCM result is consistent with that obtained by Brovkin *et al.* (1999) using an Earth-system Model of Intermediate Complexity (EMIC).

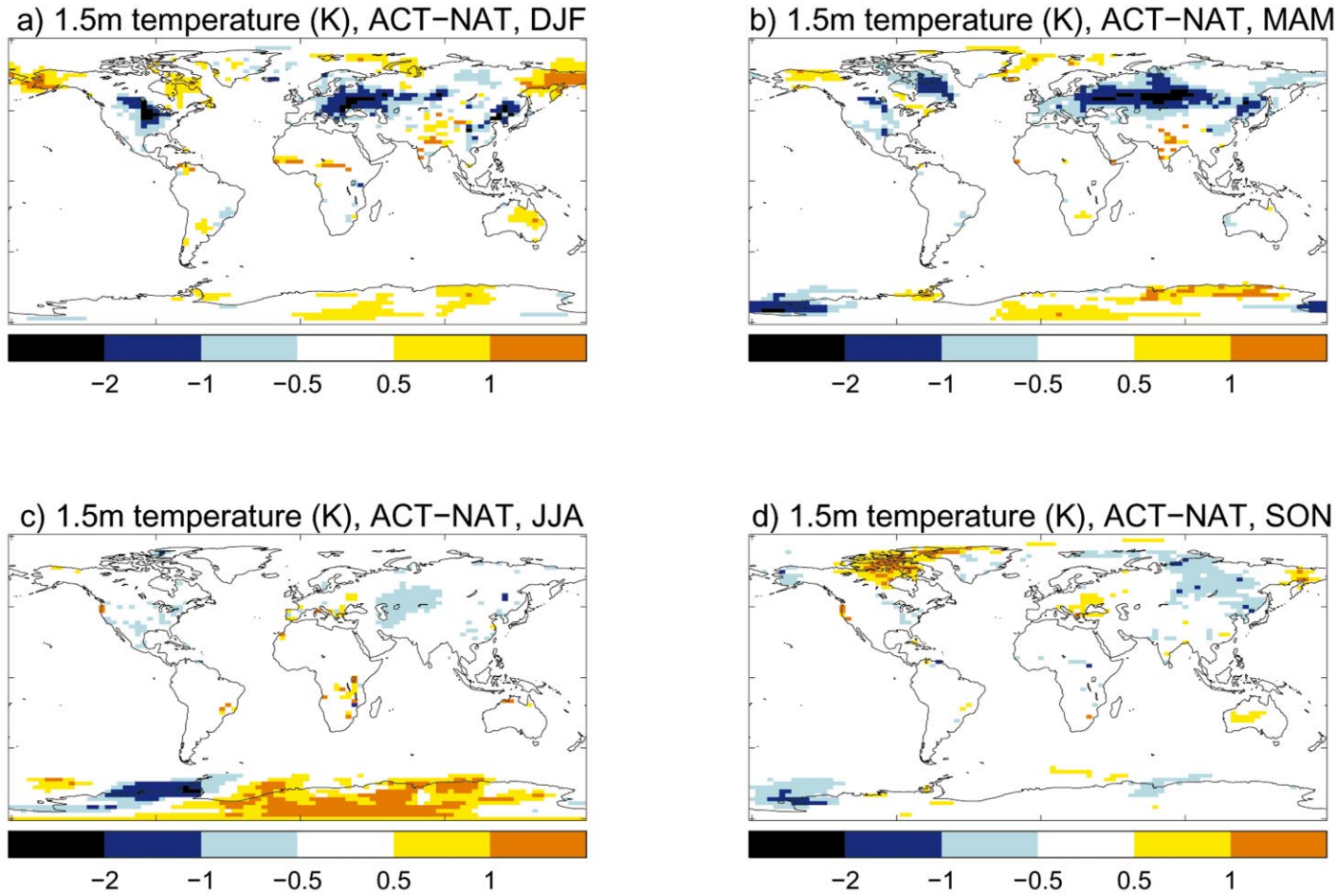

Figure 3. Twenty-year mean seasonal temperature differences between climates simulated with ACT and NAT. Differences discussed in the text were statistically significant at the 95% confidence level or better, according to a Student's *t*-test on the timeseries of means from each individual year with autocorrelation considered.

Lower temperatures were also seen with ACT relative to NAT across central and western Europe in MAM (Figure 3), despite a lack of snow cover and hence minimal albedo change in this season. These temperature differences were associated with increased cloud cover reducing the mean downward shortwave radiation flux, and were not seen when comparing the ACT climate with ALBNAT (Figure 4).

In the Sahel, dry-season (DJF) temperatures were higher with ACT than with NAT (Figure 3), with the flux of latent heat away from the surface being reduced. The contemporary agricultural vegetation had less access to the soil moisture store than the natural savanna

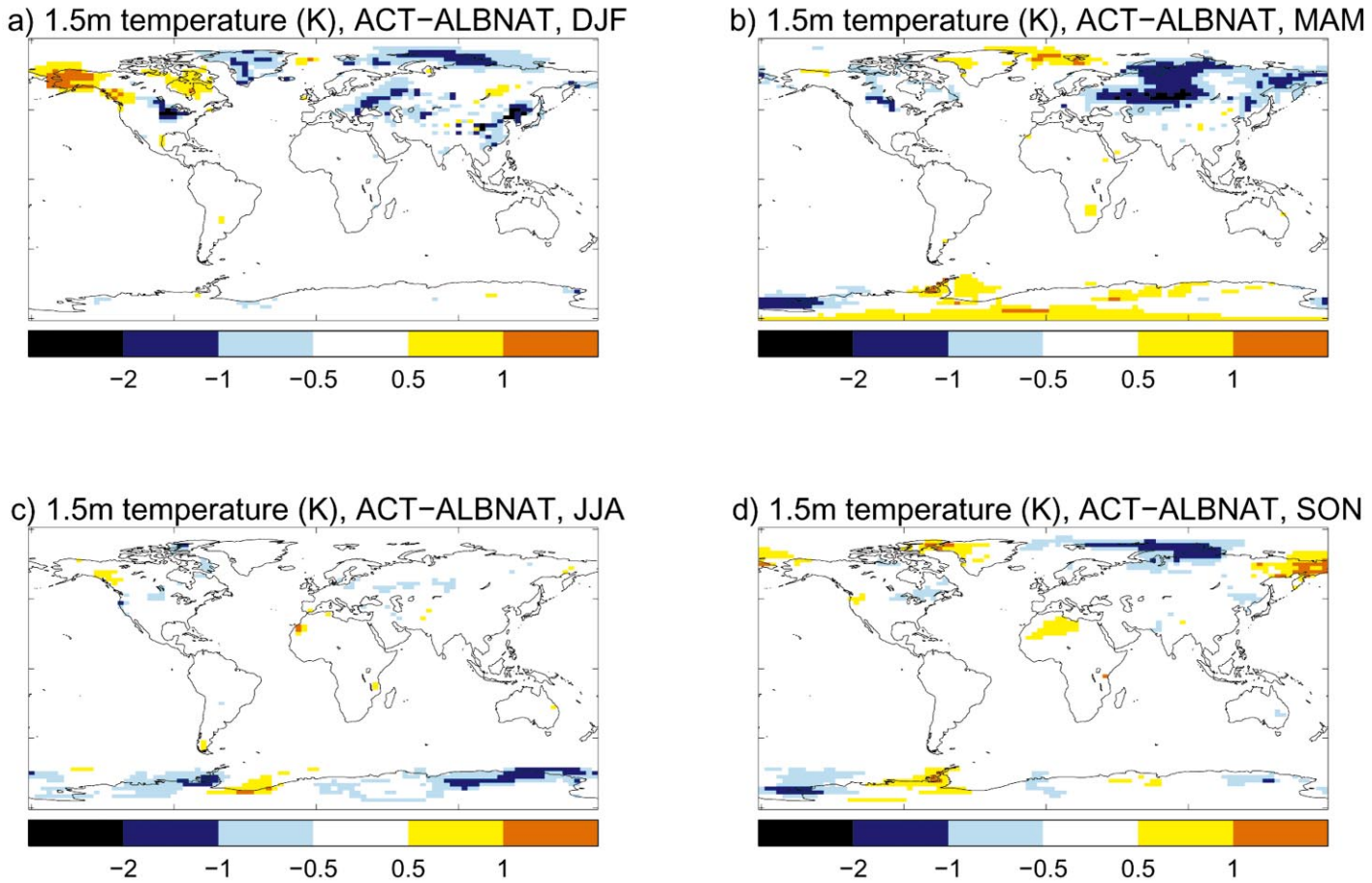

Figure 4. Twenty-year mean seasonal temperature differences between ACT climate and ALBNAT.

vegetation due to shallower mean rooting depths, so allowed less transpiration during the dry season. Similarly, the start of the Indian monsoon season (MAM) was warmer with ACT than with NAT, again with the latent heat flux being smaller with actual vegetation. In ALBNAT, the 1.5 m temperature in both the Sahel and India was similar to that simulated with ACT, indicating a negligible effect of the surface albedo change in those regions.

North-east Australia was warmer with ACT than with NAT in DJF, with reduced cloud cover and a 1 mm/day decrease in precipitation causing an increase in the downward shortwave radiation flux and a reduction in the upward latent heat flux. Although only a small area of land cover was different in the two simulations, the warm anomaly covered a much wider area and the associated precipitation reduction extended well over the Pacific Ocean, suggesting that the changes were due to a larger-scale modification to the atmospheric circulation.

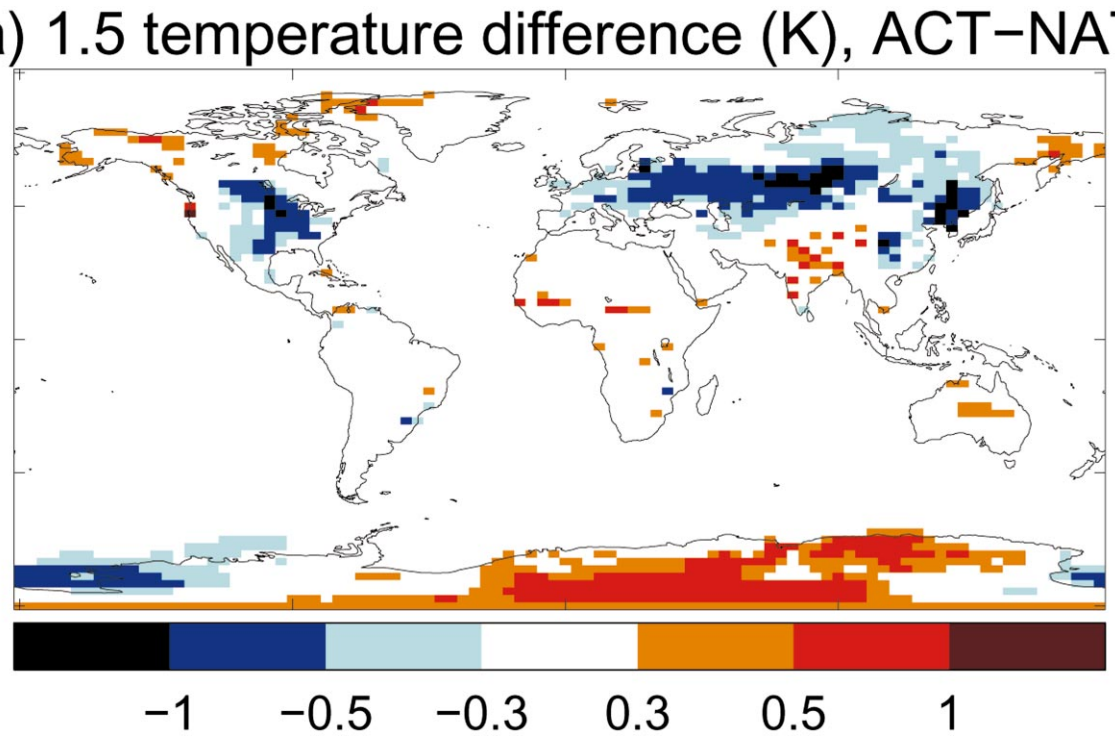

Figure 5a. Figure caption on page 11.

Mean sea-level pressure over this region was approximately 0.5 hPa higher with ACT, indicating a general decrease in ascent. Local climate changes were also seen in regions where land cover did not change at all; in western central Asia, temperatures in June, July and August (JJA) were 0.5 K to 1.0 K lower with ACT than with NAT, and over the land around the Bering Straits, temperatures were different with ACT and NAT throughout much of the year. So, as well as influencing climate in the immediate locality, large-scale land cover changes in the model influenced the global circulation and hence affected the energy and water budgets in areas in which local vegetation change was not imposed (Chase *et al.*, 2000).

The mean 1.5 m temperature over all land points was 0.06 K lower with ACT than with NAT, with a significance level of 97%, but the global land mean 1.5 m temperature in ALBNAT was not significantly different from that in the NAT climate. The results from this model therefore suggest that the surface albedo increase in temperate agricultural regions dominates the impact of present-day land use on global land temperature, with the areas warmed by reduced evaporation making a relatively minor contribution at the global scale. Consequently, diagnosis of the radiative forcing should provide a useful means of comparing past and present global land use with other influences on climate. The local annual mean shortwave radiative forcing exceeded -5 W m^2 in parts of Europe, North America and the cooler regions of Asia (Figure 5b), which is considerably greater than the forcings relative to pre-industrial times exerted by greenhouse gases (2 W/m^2)

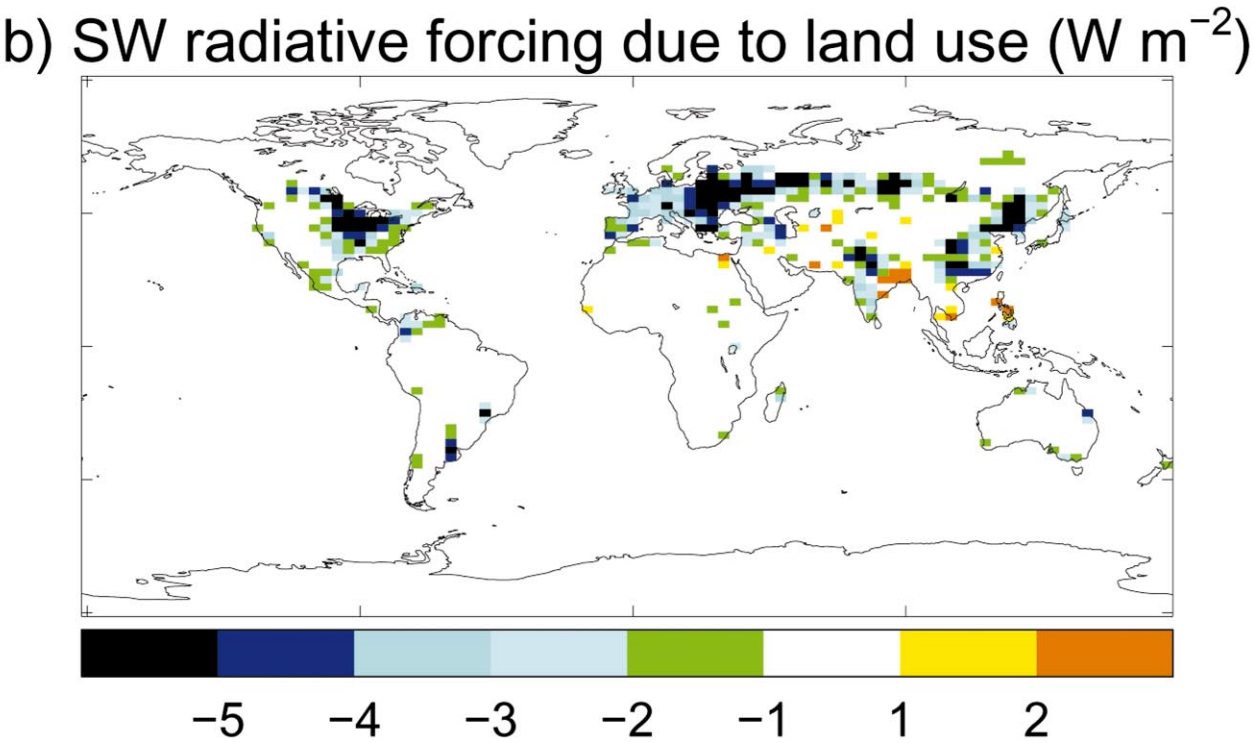

Figure 5. (a) Twenty-year annual mean temperature differences between ACT and NAT climates. (b) Mean shortwave radiative forcing due to difference in ACT and NAT albedo parameters, diagnosed in ACT climate.

and the direct effect of sulphate aerosols (-1.5 W/m^2) over these areas (Houghton *et al.*, 1995). The global mean forcing by surface albedo change was -0.20 W/m^2, which is smaller than the global forcing by greenhouse gases (2.5 W m^{-2}, Houghton *et al.*, 1995; Schimel *et al.*, 1996); whereas the greenhouse forcing is relatively uniformly distributed across the globe, the albedo changes simulated here were very localized. Nevertheless, the global surface albedo forcing is of a similar magnitude to the forcings by changes in sulphate aerosols (direct effect), stratospheric and tropospheric ozone, halocarbons, and N_2O over the industrial period (Schimel *et al.*, 1996). In comparison, Hansen *et al.* (1997) estimated the land-use forcing to be -0.40 W/m^2.

5. CONCLUSIONS

These results suggest that the main biogeophysical impact of land cover change has been a cooling influence in temperate latitudes, acting through an increase in winter and spring surface albedo. In these seasons, the 1.5m temperature simulated in the Eurasian and North American agricultural regions is up to 2 K lower with actual rather than potential vegetation, and the annual mean cooling is

approximately 0.5–1 K. Localized warming is seen in some low-latitude areas, attributable to reduced evapotranspiration. Non-local effects acting through atmospheric circulation changes are also seen. The global shortwave radiative forcing by the surface albedo change relative to pre-agricultural times is simulated to be -0.2 W/m^2, which suggests that the climatic influence of land use is comparable with that of the ''minor'' greenhouse gases and aerosols.

Approximately 50–55% of global deforestation has taken place since 1860 (Meyer, 1996), and while Europe had cleared over 80% of its agricultural area by that time, over half of forest removal in North America has taken place since. However, although the greenhouse gas emissions from land cover change have been included in GCM simulations of historical climate change, the related biogeophysical changes have so far been neglected. Since the mid-latitude cooling simulated here is of a similar magnitude to the warming observed over the industrial era, the omission of land cover change may limit the ability of these models to reproduce observed past climate changes at the regional scale. In particular, a large proportion of climate observations have been taken in areas undergoing changing land use, so GCM simulations should include land cover changes if they are to be compared against these data for the detection of anthropogenic climate change.

ACKNOWLEDGEMENTS

The author thanks S. E. Lee and F. I. Woodward for providing data from Sheffield University vegetation model, S. H. Cousins and M. Strathern for suggesting this study, and P. M. Cox, J. M. Edwards, W. J. Ingram, A. Jones, K. P. Shine, P. J. Valdes and two anonymous referees for advice and comments. This work forms part of the Climate Prediction Programme of the U.K. Department of the Environment, Transport and the Regions (Contract No. PECD 7/12/37).

REFERENCES

Betts, R. A., 1999. Self-beneficial effects of vegetation on climate in an Ocean-Atmosphere General Circulation Model. *Geophys. Res. Lett.*, **26**, 1457–1460.

Brovkin, V., Ganapolski, A., Claussen, M., Kubatzki, C. and Petoukhov, V., 1999. Modelling climate response to historical land cover change. *Global Ecol. Biogeogr.*, **8**, 509–517.

Chase, T. N., Pielke, R. A., Kittel, T. G. F., Nemani, R. R. and Running, S. W., 2000. Simulated impacts of historical land cover changes on global climate in northern winter. *Clim. Dyn.*, **16**, 93–105.

Cox, P. M., Huntingford, C. A. and Harding, R. J., 1998. A canopy conductance and photosynthesis model for use in a GCM land surface scheme. *J. Hydrol.*, **212–213**, 79–94.

Cox, P. M., Betts, R. A., Bunton, C. B., Essery, R. L. H., Rowntree, P. R. and Smith, J., 1999. The impact of new land surface physics on the GCM simulation of climate and climate sensitivity. *Clim. Dyn.*, **15**, 183–203.

Cullen, M. J. P., 1993. The unified forecast/climate model. *Meteorol. Magazine*, **122**, 81–94.

Edwards, J. M. and Slingo, A., 1996. Studies with a flexible new radiation code. I: Choosing a configuration for a large-scale model. *Quart. J. Roy. Meteor. Soc.*, **122**, 689–720.

Gregory, J. M. and Mitchell, J. F. B., 1995. Simulation of daily variability of surface temperature and precipitation over Europe in the current and $2 \times CO_2$ climates using the UKMO high-resolution climate model. *Quart. J. Roy. Meteorol. Soc.*, **121**, 1451–1476.

Gregory, D., Shutts, G. and Mitchell, J., 1998. A new gravity wave drag scheme incorporating anisotropic orography and low level wave breaking; Impact upon the climate of the UK Meteorological Office Unified Model. *Quart. J. Roy. Meteorol. Soc.*, **124**, 463–493.

Hansen, J. E., Russell, G., Rind, D., Stone, P., Lacis, A. A., Lebedeff, S., Ruedy, R. and Travis, R. L., 1983. Efficient three dimensional global models for climate studies, Models I and II. *Mon. Weather Rev.*, **111**, 609–662.

Hansen, J., Sato, M., Lacis, A. and Ruedy, R., 1997. The missing climate forcing. *Phil. Trans. R. Soc. Lond. B*, **352**, 231–240.

Haxeltine, A. and Prentice, C., 1996. Biome3: An equilibrium terrestrial biosphere model based on ecophysiological constraints, resource availability, and competition among plant functional types. *Global Biogeochem. Cycle*, **10**, 693–709.

Houghton, J. T., Filho, L. G. M., Bruce, J., Lee, H., Callander, B. A., Haites, E., Harris, N. and Maskell, K., 1995. *Climate Change 1994. Radiative Forcing of Climate Change*. Cambridge University Press, Cambridge.

Meyer, W. B., 1996. *Human Impact on the Earth*. Cambridge University Press.

Pielke, R. A., Avissar, R., Raupach, M., Dolman, A. J., Zeng, X. and Denning, A. S., 1998. Interactions between the atmosphere and terrestrial ecosystems: influence on weather and climate. *Global Change Biol.*, **4**, 461–475.

Santer, B. D., Wigley, T. M.L., Barnett, T. P. and Anyamba, E., 1996. Detection of climate change and attribution of causes. In: Houghton, J. T., Meira Filho, L. G., Callander, B. A., Harris, N., Kattenberg, A. and Maskell, K., Eds. *Climate Change 1995. The Science of Climate Change*, chapter 8. Cambridge University Press, Cambridge, 407–444.

Schimel, D., Alves, D., Enting, I., Heimann, M., Joos, F., Raynaud, D., Wigley, T., Prather, M., Derwent, R., Enhalt, D., Fraser, P., Sanhueza, E., Zhou, X., Jonas, P., Charlson, R., Rodhe, H., Sadasivan, S., Shine, K. P., Fouquart, Y., Ramaswamy, V., Solomon, S., Srinivasan, J., Albritton, D., Derwent, R., Isaksen, I., Lal, M. and Wuebbles, D., 1996. Radiative forcing of climate change. In: Houghton, J. T., Filho, L. G. M., Callander, B. A., Harris, N., Kattenberg, A. and Maskell, K., Eds. *Climate Change 1995. The Science of Climate Change*, chapter 2. Cambridge University Press, Cambridge, 65–131.

Smith, R. N. B., 1990. A scheme for predicting layer clouds and their water content in a general circulation model. *Quart. J. Roy. Met. Soc.*, **116**, 435–460.

Tett, S. F. B., Stott, P. A., Allen, M. R., Ingram, W. J. and Mitchell, J. F. B., 1999. Causes of twentieth century climate change near the Earth's surface. *Nature*, **399**, 569–572.

Thomas, G. and Rowntree, P. R., 1992. The boreal forests and climate. *Quarterly J. Roy. Meteorol. Soc.*, **118**, 469–497.

Wilson, M. F. and Henderson-Sellers, A. F., 1985. A global archive of land cover and soils data for use in general circulation climate models.. *J. Climatol.*, **5**, 119–143.

Woodward, F. I., Smith, T. M. and Emanuel, W. R., 1995. A global land primary productivity and phytogeography model. *Global Biogeochem. Cycle.*, **9**, 471–490.